

# Blind Performance Prediction for Deep Learning Based Ultra-Massive MIMO Channel Estimation

Wentao Yu<sup>†</sup>, Hengtao He<sup>†</sup>, Xianghao Yu<sup>‡</sup>, Shenghui Song<sup>†</sup>,

Jun Zhang<sup>†</sup>, *Fellow, IEEE*, and Khaled B. Letaief<sup>†</sup>, *Fellow, IEEE*

<sup>†</sup>Dept. of Electronic and Computer Engineering, Hong Kong University of Science and Technology, Hong Kong

<sup>‡</sup>Dept. of Electrical Engineering, City University of Hong Kong, Hong Kong

Email: <sup>†</sup>wyuaq@connect.ust.hk, <sup>†</sup>{eehthe, eeshsong, eejzhang, eekhaled}@ust.hk, <sup>‡</sup>alex.yu@cityu.edu.hk

**Abstract**—Reliability is of paramount importance for the physical layer of wireless systems due to its decisive impact on end-to-end performance. However, the uncertainty of prevailing deep learning (DL)-based physical layer algorithms is hard to quantify due to the black-box nature of neural networks. This limitation is a major obstacle that hinders their practical deployment. In this paper, we attempt to quantify the uncertainty of an important category of DL-based channel estimators. An efficient statistical method is proposed to make *blind* predictions for the mean squared error of the DL-estimated channel *solely* based on received pilots, without knowledge of the ground-truth channel, the prior distribution of the channel, or the noise statistics. The complexity of the blind performance prediction is low and scales only linearly with the number of antennas. Simulation results for ultra-massive multiple-input multiple-output (UM-MIMO) channel estimation with a mixture of far-field and near-field paths are provided to verify the accuracy and efficiency of the proposed method.

## I. INTRODUCTION

As the adoption of the 5-th generation (5G) wireless networks continues to accelerate throughout the world, we are witnessing exciting global research and development activities to formulate 6G as the next-generation mobile communication network. In particular, 6G is envisioned to be both a driver and a beneficiary of artificial intelligence (AI) [1]. On one hand, ubiquitous high-speed wireless links in 6G lay the foundation for emerging AI applications, such as edge intelligence, federated learning, and extended reality [2]. On the other hand, AI, in particular DL, facilitates the operation of increasingly complicated wireless systems, and has already achieved great success in the physical layer, such as data detection [3], hybrid precoding [4], [5], and channel estimation [6], [7], [8].

However, the lack of reliability guarantee is a critical concern that hinders the widespread deployment of DL-based physical layer design. Traditional physical layer algorithms, such as the least squares, have deeply rooted mathematical foundations and performance guarantees. In contrast, DL-based methods are mostly treated as black boxes [9]. Although they can learn from huge amounts of training data and achieve the state-of-the-art performance, the over-parameterized and non-transparent nature makes them hard to analyze. It is difficult to even have an idea of whether DL-based methods are working well or not in practical deployment. By taking channel estimation as an example, the commonly-adopted mean squared error (MSE) metric requires knowledge of the ground-truth channel, which is unavailable in deployment. Therefore, we can hardly identify whether the DL-based channel estimators are making mistakes, until the error has been propagated to higher levels and reveals

itself as, e.g., a decrease in the communication quality. This is certainly undesirable for the physical layer which has stringent requirements on reliability and robustness.

Given such a dilemma, it is crucial to study how to quantify the uncertainty of DL-based physical layer algorithms without the ground-truth data. Such efforts not only serve as a safeguard so that traditional algorithms can take over when mistakes are detected, but also provide valuable insights for the design of the subsequent modules in the wireless system. In addition, good performance criteria without the ground-truth data can serve as unsupervised loss functions that enable online updates of the DL-based physical layer algorithms [10]. In this study, we focus on the channel estimation problem as a starting point.

To realize these possibilities, we propose a *blind* performance prediction method for the (normalized) MSE of the estimated channel *without* any oracle information<sup>1</sup>. The proposed method is compatible with an important category of state-of-the-art DL-based channel estimators relying on approximate message passing (AMP) and its variants [6], [7], [8], [11]. The basic idea is to utilize the Gaussian error property of AMP-related algorithms together with the Stein's unbiased risk estimator (SURE) to predict the MSE performance [12]. To enable the computation of SURE, we also propose a principal component analysis (PCA)-based method to estimate the noise level from a single instance of noisy channel. Simulation results for channel estimation in UM-MIMO systems are provided to verify the accuracy and efficiency of the proposed method. To the best of the authors' knowledge, this is the first work on the uncertainty quantification of DL-based channel estimation algorithms.

Different from [13] which was proposed for the thresholding-based sparse channel denoising problems, this paper targets the more general compressed channel estimation problem, eliminates the need of sparsity, and is tailored for DL-based methods. Unlike the state evolution of AMP-related algorithms, which focuses on performance analysis and requires the oracle information [11], this paper instead targets blind performance prediction and does not require any oracle information.

**Notation:**  $\mathbf{A}^T$ ,  $\mathbf{A}^H$ ,  $\mathbf{A}^\dagger$ , and  $\text{tr}(\mathbf{A})$  are the transpose, Hermitian, pseudo-inverse, and trace of matrix  $\mathbf{A}$ , respectively.  $\|\mathbf{a}\|_p$ ,  $(\mathbf{a})_i$ , and  $\max(\mathbf{a})$  are the  $\ell_p$ -norm, the  $i$ -th element, and the maximum element of vector  $\mathbf{a}$ , respectively.  $|a|$  is the absolute value of scalar  $a$ .  $\mathbf{B} = \text{blkdiag}(\mathbf{A}_1, \mathbf{A}_2, \dots, \mathbf{A}_n)$  returns a block diagonal matrix by aligning  $\mathbf{A}_1, \mathbf{A}_2, \dots, \mathbf{A}_n$  along the diagonal.  $\mathbf{I}_N$  is an identity matrix of size  $N \times N$ .  $\mathcal{N}(\boldsymbol{\mu}, \boldsymbol{\Sigma})$  and  $\mathcal{CN}(\boldsymbol{\mu}, \boldsymbol{\Sigma})$  are respectively the real-valued and complex-valued Gaussian distributions with mean  $\boldsymbol{\mu}$  and covariance

This work was supported by the Hong Kong Research Grants Council under Grant 16209622, 16212922 and 16212120, and by the Shenzhen Science and Technology Innovation Committee under Grant SGDX20210823103201006.

<sup>1</sup>By oracle, we refer to what cannot be known in practical deployment, e.g., the ground-truth channel, the prior distribution, and the noise statistics.

$\Sigma$ .  $U(a_1, a_2)$  denotes a uniform distribution over the interval  $[a_1, a_2]$ . The divergence of a function  $f : \mathbb{R}^N \rightarrow \mathbb{R}^N$  with respect to the input  $\mathbf{x}$  is  $\text{div}_{\mathbf{x}}\{f(\mathbf{x})\} \triangleq \frac{1}{N} \sum_{i=1}^N \frac{\partial(f(\mathbf{x}))_i}{\partial(\mathbf{x})_i}$ .

## II. SYSTEM MODEL AND TECHNICAL BACKGROUND

We consider the uplink channel estimation in millimeter-wave (mmWave) or terahertz (THz) UM-MIMO systems as an example to present our proposal. We first introduce the system and channel models. A category of DL-based channel estimators relying on AMP-related algorithms is then discussed, to which the proposed blind performance prediction method is applicable. We later formulate the problem, and transform it to a more tractable form via the Gaussian error property of AMP.

### A. System and Channel Models

Consider the uplink of a UM-MIMO system where the base station (BS) is equipped with a uniform planar array (UPA) with  $\sqrt{N} \times \sqrt{N}$  antennas and  $N_{\text{RF}}$  radio frequency (RF) chains to serve  $K$  single-antenna user equipments (UEs). To enhance the energy efficiency, a partially-connected hybrid analog-digital structure is adopted at the BS, where each RF chain is connected with  $N/N_{\text{RF}}$  antennas [5]. The carrier frequency, carrier wavelength, antenna spacing, and the speed of light are denoted as  $f_c$ ,  $\lambda_c$ ,  $d_a$ , and  $c$ , respectively.

The spatial-frequency channel  $\tilde{\mathbf{h}} \in \mathbb{C}^{N \times 1}$  of mmWave/THz UM-MIMO systems can be characterized by the superposition of one line-of-sight (LoS) and  $L - 1$  non-LoS paths [6], i.e.,

$$\tilde{\mathbf{h}} = \sum_{l=1}^L \alpha_l \mathbf{a}(\phi_l, \theta_l, r_l) e^{-j2\pi f_c \tau_l}, \quad (1)$$

where  $\alpha_l$ ,  $\mathbf{a}(\phi_l, \theta_l, r_l) \in \mathbb{C}^{N \times 1}$ , and  $\tau_l$  denote the path loss, array response, and time delay of the  $l$ -th path, respectively. The array response  $\mathbf{a}(\phi_l, \theta_l, r_l)$  is determined by the azimuth angle-of-arrival (AoA)  $\phi_l$ , the elevation AoA  $\theta_l$ , and the distance  $r_l$  of the  $l$ -th path. Due to the joint effects of large array aperture and small wavelength, the near-field region becomes non-negligible in mmWave/THz UM-MIMO systems [6], [14]. The array response, considering both far-field (planar-wave) and near-field (spherical-wave) paths, is given by

$$\mathbf{a}(\phi_l, \theta_l, r_l) = \begin{cases} \mathbf{a}^{\text{far}}(\phi_l, \theta_l, r_l), & \text{if } r_l > D_{\text{Rayleigh}}, \\ \mathbf{a}^{\text{near}}(\phi_l, \theta_l, r_l) & \text{otherwise.} \end{cases} \quad (2)$$

Here  $\mathbf{a}^{\text{far}}$  and  $\mathbf{a}^{\text{near}}$  are respectively the far- and near-field array responses, and  $D_{\text{Rayleigh}} = \frac{2D^2}{\lambda_c}$  represents the Rayleigh distance, i.e., the boundary between the far and near fields, with  $D$  denoting the array aperture. The detailed derivation of  $\mathbf{a}^{\text{far}}$  and  $\mathbf{a}^{\text{near}}$  can be found in [6] and is omitted here for brevity.

In the uplink training phase, the UEs send known pilots to the BS for  $Q$  time slots. Assuming that the widely-used orthogonal pilots are adopted, we consider an arbitrary UE without loss of generality. The received pilot signal  $\mathbf{y}_q \in \mathbb{C}^{N_{\text{RF}} \times 1}$  at the BS in time slot  $q$  is given by

$$\tilde{\mathbf{y}}_q = \mathbf{W}_{\text{BB},q}^H \mathbf{W}_{\text{RF},q}^H \tilde{\mathbf{h}} s_q + \mathbf{W}_{\text{BB},q}^H \mathbf{W}_{\text{RF},q}^H \tilde{\mathbf{n}}_q, \quad (3)$$

where  $\mathbf{W}_{\text{BB},q} \in \mathbb{C}^{N_{\text{RF}} \times N_{\text{RF}}}$  is the digital combiner,  $\mathbf{W}_{\text{RF},q} \in \mathbb{C}^{N \times N_{\text{RF}}}$  is the analog combiner,  $s_q$  is the pilot symbol that is set as 1, and  $\tilde{\mathbf{n}}_q \in \mathbb{C}^{N \times 1}$  is the additive white Gaussian noise (AWGN) vector following  $\mathcal{CN}(\mathbf{0}, \sigma_{\tilde{\mathbf{n}}}^2 \mathbf{I}_N)$ . Due to the partially-connected structure, we have that  $\mathbf{W}_{\text{RF},q} = \text{blkdiag}(\mathbf{w}_{1,q}, \mathbf{w}_{2,q}, \dots, \mathbf{w}_{N_{\text{RF}},q})$ , where each element of the

vector  $\mathbf{w}_{i,q} \in \mathbb{C}^{N/N_{\text{RF}} \times 1}$  is picked from one-bit quantized angles, i.e.,  $(\mathbf{w}_{i,q})_j \in \sqrt{\frac{N_{\text{RF}}}{N}} \{\pm 1\}$  [6]. To whiten the effective noise, we set the digital combiner as  $\mathbf{W}_{\text{BB},q} = \mathbf{D}_q^{-1}$ , where  $\mathbf{D}_q$  is an upper triangular matrix and  $\mathbf{D}_q^H \mathbf{D}_q$  is the Cholesky decomposition of matrix  $\mathbf{W}_{\text{RF},q}^H \mathbf{W}_{\text{RF},q}$ . The received pilot  $\tilde{\mathbf{y}} = [\tilde{\mathbf{y}}_1^T, \tilde{\mathbf{y}}_2^T, \dots, \tilde{\mathbf{y}}_Q^T]^T \in \mathbb{C}^{QN_{\text{RF}} \times 1}$  of  $Q$  time slots is  $\tilde{\mathbf{y}} = \tilde{\mathbf{M}}\tilde{\mathbf{h}} + \tilde{\mathbf{n}}$ , where  $\tilde{\mathbf{M}} = [(\mathbf{W}_{\text{BB},1}^H \mathbf{W}_{\text{RF},1}^H)^T, \dots, (\mathbf{W}_{\text{BB},Q}^H \mathbf{W}_{\text{RF},Q}^H)^T]^T \in \mathbb{C}^{QN_{\text{RF}} \times N}$ , and  $\tilde{\mathbf{n}} \in \mathbb{C}^{QN_{\text{RF}} \times 1}$  is the whitened effective noise following  $\mathcal{CN}(\mathbf{0}, \sigma_{\tilde{\mathbf{n}}}^2 \mathbf{I}_{QN_{\text{RF}}})$ . The system model can be transformed to its equivalent real-valued form by stacking the real and imaginary parts [6], [8], i.e.,

$$\mathbf{y} = \mathbf{M}\mathbf{h} + \mathbf{n}, \quad (4)$$

with  $\mathbf{y}, \mathbf{n} \in \mathbb{R}^{2QN_{\text{RF}} \times 1}$ ,  $\mathbf{M} \in \mathbb{R}^{2QN_{\text{RF}} \times 2N}$ , and  $\mathbf{h} \in \mathbb{R}^{2N \times 1}$ . The goal is to estimate the channel  $\mathbf{h}$  from the received signal  $\mathbf{y}$  and the measurement matrix  $\mathbf{M}$ , where the dimension of  $\mathbf{y}$  is usually smaller than that of  $\mathbf{h}$ , i.e.,  $QN_{\text{RF}} < N$ , due to the requirement of low pilot overhead<sup>2</sup>. To solve the problem, AMP and related algorithms have attracted great interest due to the low computational complexity and the tractable error dynamics via the state evolution [11], [15]. Many efficient DL-based estimators are developed based on them and achieved promising performance [6], [8], [7], to which the proposed blind prediction method can be effectively applied.

### B. DL-Based Channel Estimators Relying on AMP

AMP is an efficient algorithm for compressed sensing-based channel estimation and works for an independent and identically distributed (i.i.d.) sub-Gaussian measurement matrix  $\mathbf{M}$ . The per-iteration update rules of AMP consist of a linear estimator (LE) and a non-linear estimator (NLE) [11], given by

$$\begin{aligned} \text{AMP-LE:} \quad \mathbf{r}^{(t)} &= \mathbf{h}^{(t)} + \mathbf{M}^T(\mathbf{y} - \mathbf{M}\mathbf{h}^{(t)}) + \mathbf{r}_{\text{Onsager}}^{(t)}, \\ \text{AMP-NLE:} \quad \mathbf{h}^{(t+1)} &= \eta_t(\mathbf{r}^{(t)}), \end{aligned} \quad (5)$$

where the superscript  $(t)$  indicates the  $t$ -th iteration, and  $\mathbf{r}_{\text{Onsager}}^{(t)} = \frac{N}{QN_{\text{RF}}} \text{div}_{\mathbf{r}^{(t)}}\{\eta_t(\mathbf{r}^{(t)})\}(\mathbf{r}^{(t-1)} - \mathbf{h}^{(t-1)})$  is the Onsager correlation term that ensures the input of the NLE is the ground-truth channel  $\mathbf{h}$  corrupted by AWGN, i.e.,  $\mathbf{r}^{(t)} = \mathbf{h} + \mathbf{e}^{(t)}$ , where  $\mathbf{e}^{(t)} \sim \mathcal{N}(\mathbf{0}, \sigma_{\mathbf{e}^{(t)}}^2 \mathbf{I}_{2N})$  holds, and  $\eta_t(\cdot)$  is a Lipschitz-continuous function [11]. Orthogonal AMP (OAMP) is an extension that eliminates the Onsager correlation and is compatible with a wider range of measurement matrices [15], [11]. The per-iteration update rules of OAMP can be summarized as

$$\begin{aligned} \text{OAMP-LE:} \quad \mathbf{r}^{(t)} &= \mathbf{h}^{(t)} + \mathbf{W}^{(t)}(\mathbf{y} - \mathbf{M}\mathbf{h}^{(t)}), \\ \text{OAMP-NLE:} \quad \mathbf{h}^{(t+1)} &= \eta_t(\mathbf{r}^{(t)}), \end{aligned} \quad (6)$$

where the LE is constructed to be de-correlated and the NLE is designed to be a divergence-free function [15]. We say that the LE is de-correlated when  $\text{tr}(\mathbf{I}_{2N} - \mathbf{W}^{(t)}\mathbf{M}) = 0$  holds. The matrix  $\mathbf{W}^{(t)} \in \mathbb{R}^{2N \times 2QN_{\text{RF}}}$  is built upon either the matched filter, the pseudo-inverse, or the linear minimum MSE (LMMSE) estimators [15]. The divergence-free NLE can be constructed from an arbitrary function by subtracting its divergence [15]. Similar to AMP, OAMP can also guarantee that the input of

<sup>2</sup>In this paper, we focus on the compressed sensing-based channel estimation, i.e.,  $QN_{\text{RF}} < N$ . Nevertheless, both AMP-related algorithms and the proposed blind performance prediction method can also be applied when  $QN_{\text{RF}} \geq N$ .

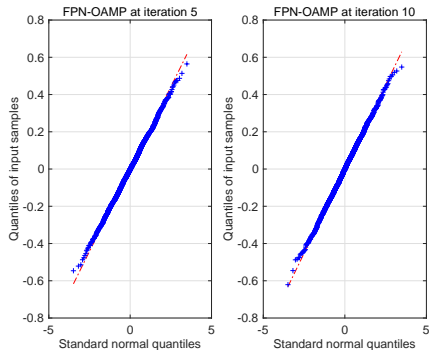


Fig. 1. QQ plot of the NLE input error evaluated at iterations 5 and 10 of the FPN-OAMP algorithm when SNR equals 15 dB. The plots show that the error follows zero-mean Gaussian distribution due to the de-correlated LE.

the NLE equals  $\mathbf{r}^{(t)} = \mathbf{h} + \mathbf{e}^{(t)}$  with  $\mathbf{e}^{(t)} \sim \mathcal{N}(\mathbf{0}, \sigma_{\mathbf{e}^{(t)}}^2 \mathbf{I}_{2N})$ , i.e., the ground-truth channel  $\mathbf{h}$  corrupted by AWGN [15].

An important property of the AMP and OAMP is that the NLE can be interpreted as a Gaussian noise denoiser [16]. Therefore, powerful DL-based denoisers could be incorporated to enhance the performance. Empirical results in the literature showed that the Gaussian error property still holds even if black-box denoisers are utilized, such as neural networks [7], [16]. The proposed blind performance predictor is established only based on the Gaussian error property, which can be easily satisfied by a range of AMP-related algorithms [11] and their DL-based variants, indicating its wide applicability.

As an example, we verify the Gaussian error property of our previously proposed FPN-OAMP algorithm [6], [17]. Specifically, it adopts a de-correlated LE based on the pseudo-inverse matrix, i.e.,  $\mathbf{W}^{(t)} = \frac{2N}{\text{tr}(\mathbf{M}^\dagger \mathbf{M})} \mathbf{M}^\dagger$ , and a convolutional neural network-based NLE, i.e.,  $\eta_t(\cdot) = R_\theta(\cdot)$ , whose weights  $\theta$  are identical in each iteration. The update rules of FPN-OAMP are basically the same as (6) with guaranteed convergence [6]. The details of the dataset, the training process, and the neural architecture are deferred to Section IV. In Fig. 1, we provide the quantile-quantile (QQ) plots of the NLE input error of the FPN-OAMP algorithm evaluated at iterations 5 and 10 when the received SNR is 15 dB. It can be observed that the quantiles fall on the diagonal reference line, confirming that the NLE input error is Gaussian distributed for DL-based channel estimators relying on AMP-related algorithms. Similar results were also illustrated and discussed in the literature [7].

### C. Problem Formulation and Transformation

The target of the blind performance prediction is the MSE of the estimated channel  $\mathbf{h}^{(t+1)}$  in each iteration, defined as

$$MSE^{(t)} = \|\mathbf{h}^{(t+1)} - \mathbf{h}\|_2^2 = \|\eta_t(\mathbf{r}^{(t)}) - \mathbf{h}\|_2^2. \quad (7)$$

We cannot directly compute it since the ground-truth channel  $\mathbf{h}$  is unknown in practical deployment. Instead, we want to derive a prediction of it without using any oracle information. Based on the Gaussian error property discussed before, we have

$$\mathbf{r}^{(t)} = \mathbf{h} + \mathbf{e}^{(t)}, \quad (8)$$

which is the ground-truth channel corrupted by some AWGN. Therefore, the original problem can be transformed to predicting the MSE of a denoising problem with the DL-based denoiser  $\eta_t(\cdot)$ , where the ground-truth channel  $\mathbf{h}$ , the prior

distribution of the channel, and the variance of the noise  $\sigma_{\mathbf{e}^{(t)}}^2$ , are all unknown. The only available information in (8) is the AWGN corrupted channel  $\mathbf{r}^{(t)}$ , which can be computed solely based on the received signal  $\mathbf{y}$  and the measurement matrix  $\mathbf{M}$ .

Based on (8), we notice that  $\mathbf{r}^{(t)}$  can actually be interpreted as a Gaussian random variable, i.e.,  $\mathbf{r}^{(t)} \sim \mathcal{N}(\mathbf{h}, \sigma_{\mathbf{e}^{(t)}}^2 \mathbf{I}_{2N})$ . The function of the denoiser,  $\eta_t(\cdot)$ , is to estimate the mean  $\mathbf{h}$  of the Gaussian random variable  $\mathbf{r}^{(t)}$ . The MSE of such an estimation can be predicted based on the seminal work of Stein [12]. In the following, we tackle the blind performance prediction problem based on SURE [12] and PCA.

## III. BLIND PERFORMANCE PREDICTION

SURE is an unbiased estimate of the MSE of an estimator for the mean of a multivariate Gaussian random variable. We first present the main theorem of SURE using the notation from our setting, and then discuss the difficulties in applying it for blind performance prediction and the ways to resolve them.

**Theorem 1** ([12], [18]). *Given  $\mathbf{r}^{(t)}$ ,  $\mathbf{e}^{(t)}$  and  $\eta_t(\cdot)$  as defined in (8), the  $SURE^{(t)}$  corresponding to  $\eta_t(\mathbf{r}^{(t)})$  is a random variable specified by the following equation,*

$$SURE^{(t)} = \|\eta_t(\mathbf{r}^{(t)}) - \mathbf{r}^{(t)}\|_2^2 - 2N\sigma_{\mathbf{e}^{(t)}}^2 + 2\sigma_{\mathbf{e}^{(t)}}^2 \text{div}_{\mathbf{r}^{(t)}}(\eta_t(\mathbf{r}^{(t)})), \quad (9)$$

which is an unbiased estimator of the MSE defined in (7), i.e.,

$$\mathbb{E}_{\mathbf{e}^{(t)}}[SURE^{(t)}] = MSE^{(t)}. \quad (10)$$

*Proof:* Please refer to the proof of [18, Theorem 1]. ■

We refer to the three terms on the right-hand-side of (9) as the fidelity, variance, and divergence terms, respectively. The theorem states that the expectation of  $SURE^{(t)}$  is equal to  $MSE^{(t)}$ , without the knowledge of the ground-truth channel  $\mathbf{h}$ . In addition, thanks to the law of large numbers, if the dimension of  $\mathbf{r}^{(t)}$ , i.e.,  $2N$ , is sufficiently large, the variance of  $SURE^{(t)}$  will decrease in proportion to  $1/2N$ , and will asymptotically converge to  $MSE^{(t)}$  as the number of antennas increases, i.e.,  $\lim_{N \rightarrow \infty} SURE^{(t)} = MSE^{(t)}$  [19]. For the considered UM-MIMO systems equipped with thousands of antennas, using  $SURE^{(t)}$  as a surrogate for  $MSE^{(t)}$  can provide accurate blind performance prediction, as will be shown in Section IV.

The difficulties in applying SURE for blind performance prediction come from two aspects. First, the variance term  $\sigma_{\mathbf{e}^{(t)}}^2$  is unknown, which should also be estimated from the AWGN corrupted channel  $\mathbf{r}^{(t)}$ . Second, the divergence of the DL-based NLE,  $\eta_t(\cdot)$ , can hardly be calculated in closed form since it is not a component-wise function. We resolve the first difficulty by using a PCA-based algorithm, while tackling the second issue by an efficient Monte-Carlo method. Since the fidelity term can be directly calculated based on  $\mathbf{r}^{(t)}$  and  $\eta_t(\cdot)$ , we mainly focus on computing the variance and divergence terms.

### A. The Variance Term

The AMP and OAMP algorithms provide intuitive ways to track the variance term  $\sigma_{\mathbf{e}^{(t)}}^2$  [15]. However, they both depend on the statistics of the environmental noise, i.e.,  $\sigma_{\mathbf{h}}^2$ , which requires a dedicated training phase to estimate and may not be accurately known in practice. In addition, the accuracy of these methods is poor when DL-based components are involved, which will be shown by simulations in Section IV.

We instead propose to estimate the noise level directly based on the AWGN corrupted channel  $\mathbf{r}^{(t)} \sim \mathcal{N}(\mathbf{h}, \sigma_{\mathbf{e}^{(t)}}^2 \mathbf{I}_{2N})$ , which is the only available information in (8). Since the mean, i.e., the

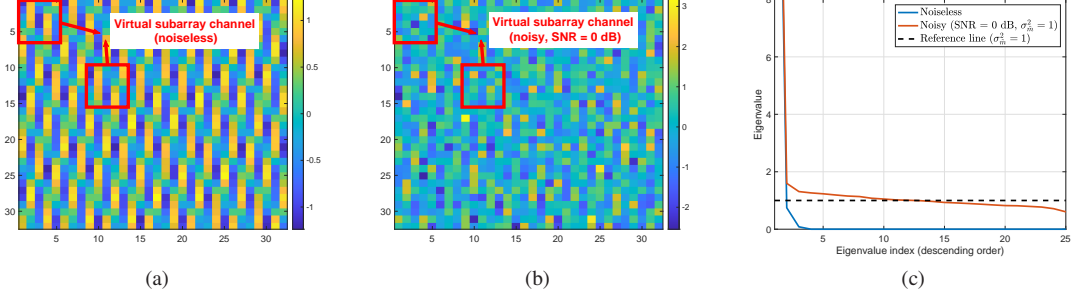


Fig. 2. (a) Heatmap of the real part of the noiseless channel. (b) Heatmap of the real part of the noisy channel corrupted by AWGN with 0 dB SNR ( $\sigma_m^2 = 1$ ). (c) Eigenvalues of the covariance matrices of the noiseless and noisy virtual subarray channels in descending order. The illustrated channel has  $L = 3$  paths.

ground-truth channel  $\mathbf{h}$ , is *unknown*, the problem is essentially to estimate the noise variance  $\sigma_{e^{(t)}}^2$  from a *single* realization of a multivariate Gaussian distribution with *unknown* mean. This is *intractable* if the channel  $\mathbf{h}$  does not have any structure.

To exploit the structural information, previous work proposed to transform the AWGN corrupted channel  $\mathbf{r}^{(t)}$  into its sparse angular-domain representation and estimate the noise variance with median absolute deviation [13]. However, for a practical UM-MIMO channel with both far- and near-field paths, the angular-domain channel is no longer sparse [6], which greatly degrades the accuracy of [13]. Therefore, we need to exploit other structural information that generally holds for the UM-MIMO channel. Specifically, we turn to the low-dimensional structure of the channel due to the limited number of paths and adopt a PCA-based method as shown in **Algorithm 1**.

To explain the ideas behind, we generate a noisy UM-MIMO channel with  $L = 3$  paths and  $N = 1024$  antennas with  $\tilde{\mathbf{h}}_{\text{noisy}} = \tilde{\mathbf{h}} + \tilde{\mathbf{m}}$  and  $\tilde{\mathbf{m}} \sim \mathcal{CN}(\mathbf{0}, \sigma_m^2 \mathbf{I}_N)$ . We set  $\sigma_m^2 = 1$  such that the SNR, defined as  $1/\sigma_m^2$ , equals 0 dB. We reshape both  $\tilde{\mathbf{h}}_{\text{noisy}}$  and  $\tilde{\mathbf{h}}$  into  $\sqrt{N} \times \sqrt{N}$  matrices and respectively plot their real parts, as shown in Fig. 2(a)(b). We then explain the algorithm line by line with this visualized example.

In lines 3 and 4, we take multiple virtual subarray channels (VSCs) from the UM-MIMO channel using a sliding window, as shown by red squares in Fig. 2(a)(b). Since the noise is white Gaussian, estimating the noise level for VSCs is equivalent to estimating that for the original channel. Therefore, we resort to the statistical properties of the VSCs instead.

In lines 5 to 7, we first calculate the covariance matrix  $\Sigma$  of the noisy VSCs, and then compute the eigenvalues of  $\Sigma$  and list them in descending order. In this process, each VSC is treated as a data point in the PCA, and the eigenvalues of  $\Sigma$  reflect the strength of the different components. We plot the eigenvalues of the clean and noisy channels in Fig. 2(c). One can see that the clean channel only has  $L = 3$  non-zero eigenvalues, equal to the number of paths. By contrast, the eigenvalues of the noisy channel are long-tailed and surround the variance of the additive noise, as shown by the reference line.

In lines 8 to 14, we split the eigenvalues into the principal and redundant dimensions, and estimate the noise level based on the latter, because it was proved in [20, Lemma 1] that the redundant eigenvalues follow  $\mathcal{N}(\sigma_m^2/2, \sigma_m^4/2s)$  when  $s$  is large enough. However, the problem is that the range of the principal dimensions, i.e., the number of paths  $L$ , is unknown in practical deployment. We adopt an iteration to split the dimensions, and stop the iteration when the mean and median of the redundant

---

### Algorithm 1 PCA-based noise level estimation

---

- 1: **Input:** AWGN corrupted channel  $\tilde{\mathbf{h}}_{\text{noisy}} \in \mathbb{C}^{N \times 1}$ , size of the virtual subarray  $\sqrt{d} \times \sqrt{d}$
  - 2: **Output:** Estimated noise level  $\hat{\sigma}_{\tilde{\mathbf{m}}}$
  - 3: Reshape  $\tilde{\mathbf{h}}_{\text{noisy}} \in \mathbb{C}^{N \times 1}$  into the equivalent real-valued tensor form  $\mathbf{H}_{\text{noisy}} \in \mathbb{R}^{\sqrt{N} \times \sqrt{N} \times 2}$
  - 4: Decompose  $\mathbf{H}_{\text{noisy}}$  into virtual subarray channels  $\{\mathbf{h}_{\text{noisy},t} \in \mathbb{R}^{2d \times 1}\}_{t=1}^s$  by sliding window, with  $s = (\sqrt{N} - \sqrt{d} + 1)^2$
  - 5: Calculate the mean vector of the virtual subarray channels, i.e.,  $\boldsymbol{\mu} = \frac{1}{s} \sum_{t=1}^s \mathbf{h}_{\text{noisy},t} \in \mathbb{R}^{2d \times 1}$
  - 6: Calculate the covariance of the virtual subarray channels, i.e.,  $\Sigma = \frac{1}{s} \sum_{t=1}^s (\mathbf{h}_{\text{noisy},t} - \boldsymbol{\mu})(\mathbf{h}_{\text{noisy},t} - \boldsymbol{\mu})^T \in \mathbb{R}^{2d \times 2d}$
  - 7: Calculate the eigenvalues  $\{\lambda_i\}_{i=1}^{2d}$  of the covariance  $\Sigma$ , and sort them in descending order, i.e.,  $\lambda_1 \geq \lambda_2 \geq \dots \geq \lambda_{2d}$
  - 8: Iteratively split the eigenvalues  $\{\lambda_i\}_{i=1}^{2d}$  into the principal and the redundant dimensions, and estimate the noise level based on the eigenvalues of the redundant dimensions:
  - 9: **for**  $i = 1 : 2d$  **do**
  - 10:      $\tau = \frac{1}{2d-i+1} \sum_{j=i}^{2d} \lambda_j$
  - 11:     **if**  $\tau$  is the median of  $\{\lambda_j\}_{j=i}^{2d}$  **then**
  - 12:          $\hat{\sigma}_{\tilde{\mathbf{m}}} = \sqrt{2\tau}$  **and break**
  - 13:     **end if**
  - 14: **end for**
- 

eigenvalues in the current iteration are found equal [20]. Then the median is used to estimate the noise level.

In blind performance prediction,  $\mathbf{r}^{(t)}$  is the same as the noisy channel mentioned above. The algorithm can thus be similarly applied to calculate the variance term  $\sigma_{e^{(t)}}^2$ .

### B. The Divergence Term

As defined in Section I, the divergence needs to take into account the effect of each element of the input vector. However, the DL-based NLE, i.e.,  $\eta_t(\cdot)$ , is not a component-wise function, which makes closed-form computation of the divergence term infeasible. In [19], the authors proved that for bounded function  $\eta_t(\cdot)$ , the divergence can be expressed as

$$\text{div}_{\mathbf{r}^{(t)}}(\eta_t(\mathbf{r}^{(t)})) = \lim_{\epsilon \rightarrow 0} \mathbb{E}_{\boldsymbol{\delta}} \left[ \frac{\boldsymbol{\delta}^T}{\epsilon} (\eta_t(\mathbf{r}^{(t)} + \epsilon \boldsymbol{\delta}) - \eta_t(\mathbf{r}^{(t)})) \right], \quad (11)$$

where  $\boldsymbol{\delta} \sim \mathcal{N}(\mathbf{0}, \mathbf{I}_{2N})$  is a Gaussian distributed random variable independent of  $\mathbf{r}^{(t)}$ , and  $\epsilon \boldsymbol{\delta}$  is a slight perturbation to the input of the function  $\eta_t(\cdot)$ . This is a powerful result compatible with

the considered DL-based NLE, since the expression in (11) does not require the explicit expression of  $\eta_t(\cdot)$ , but rather the output of it. The remaining difficulty is that expectation also does not have a closed form and cannot be computed directly. Thanks to the law of large numbers, it can be efficiently approximated via Monte-Carlo sampling. Owing to the high dimensionality of the UM-MIMO channel, a single sample of  $\delta$  is good enough to approximate the expectation in (11) by setting  $\epsilon$  as a small value [19]. We use  $\epsilon = \frac{\max(\mathbf{r}^{(t)})}{100}$  throughout this work. Overall, the approximation can be computed by

$$\text{div}_{\mathbf{r}^{(t)}}(\eta_t(\mathbf{r}^{(t)})) \approx \frac{\delta^T}{\epsilon}(\eta_t(\mathbf{r}^{(t)} + \epsilon\delta) - \eta_t(\mathbf{r}^{(t)})), \quad (12)$$

which is easy to implement and provides competitive empirical performance according to the simulations in Section IV.

### C. Complexity Analysis

We separately analyze the complexity of the fidelity, variance, and divergence terms. For the fidelity term, the complexity of computing the  $\ell_2$ -norm is  $\mathcal{O}(N)$ . For the variance term, we analyze the complexity of **Algorithm 1** step by step. The complexity of the virtual subarray decomposition in line 4 is  $\mathcal{O}(sd)$ . Computing the mean and covariance in lines 5 and 6 costs  $\mathcal{O}(sd)$  and  $\mathcal{O}(sd^2)$ , respectively. The complexity of the eigenvalue decomposition in line 7 is  $\mathcal{O}(d^3)$ , while sorting the eigenvalues costs  $\mathcal{O}(d^2)$ . The eigenvalue splitting and the noise level estimation from lines 8 to 14 costs  $\mathcal{O}(d^2)$ . Since in UM-MIMO systems  $s \approx N$  holds, the complexity of calculating the variance term is roughly  $\mathcal{O}(Nd^2 + d^3)$ . For the divergence term, the complexity lies in an additional forward propagation of the DL-based NLE  $\eta_t(\cdot)$ . This incurs a constant complexity once  $\eta_t(\cdot)$  is determined, which we denote as  $\mathcal{O}(p)$  [6]. Therefore, the total complexity of the blind performance prediction method is  $\mathcal{O}(Nd^2 + d^3 + p)$ , which scales only linearly with the number of antennas. This makes the algorithm friendly with UM-MIMO systems with potentially thousands of antennas.

## IV. SIMULATION RESULTS

### A. Simulation Setup

In the following, we verify the accuracy of the proposed blind performance prediction method with the uplink channel estimation in mmWave UM-MIMO<sup>3</sup> systems based on the FPN-OAMP algorithm [6]. We first introduce the system settings and the details of the algorithm. The main system parameters are set as  $N = 1024$ ,  $N_{\text{RF}} = 4$ ,  $L = 3$ ,  $f_c = 14$  GHz,  $d_a = 0.5\lambda_c$ ,  $Q = 128$ ,  $\theta_l \sim \mathcal{U}(-\pi/2, \pi/2)$ , and  $\phi_l \sim \mathcal{U}(-\pi, \pi)$ . In this case, the Rayleigh distance  $D_{\text{Rayleigh}}$  is about 20 meters. We set the path length as  $r_l \sim \mathcal{U}(5, 30)$  meters to model the mixture of far-field and near-field paths contained in the UM-MIMO channel. In addition, for the LoS path, we set the path loss as  $\alpha_l \sim \mathcal{CN}(0, 1)$ , while for the non-LoS paths, the path loss is set as  $\alpha_l \sim \mathcal{CN}(0, 0.1)$ . We normalize the channel  $\tilde{\mathbf{h}}$  such that  $\|\tilde{\mathbf{h}}\|_2^2 = N$ , and define the received SNR as  $1/\sigma_{\tilde{\mathbf{m}}}^2$ .

Following Section II-B, the DL-based NLE  $\eta_t(\cdot) = R_{\theta}(\cdot)$  of FPN-OAMP [6] first reshapes  $\mathbf{r}^{(t)}$  into tensor form  $\mathbf{R}^{(t)} \in \mathbb{R}^{\sqrt{N} \times \sqrt{N} \times 2}$ , and then passes it to a  $3 \times 3$  convolution (Conv) layer to upsample the input to 64 feature maps. These feature

<sup>3</sup>In the literature, UM-MIMO usually refers to systems equipped with 1024 or more antennas. Nevertheless, the proposed blind performance prediction is also observed to work well with moderate-sized massive MIMO systems with, e.g., 128 or 256 antennas. Theoretical analysis on the impact of the array size to the prediction accuracy is left as future work.

TABLE I  
PERFORMANCE OF THE NOISE LEVEL ESTIMATION

$\sigma_{\tilde{\mathbf{m}}}$ (SNR)	Method	Bias	Std	RMSE	Runtime (s)
0.5623 (5 dB)	Oracle	0.0001	0.0089	0.0089	0.0001
	<b>Proposed</b>	0.0038	0.0128	0.0134	0.0039
	Sparsity	0.0396	0.0233	0.0459	0.0007
0.1778 (15 dB)	Oracle	0.0001	0.0027	0.0027	0.0001
	<b>Proposed</b>	0.0015	0.0039	0.0042	0.0039
	Sparsity	0.0367	0.0207	0.0422	0.0007
0.0562 (25 dB)	Oracle	<0.0001	0.0009	0.0009	0.0001
	<b>Proposed</b>	0.0004	0.0012	0.0013	0.0038
	Sparsity	0.0391	0.0237	0.0457	0.0007

maps further go through a ResNet-like structure consisting of three residual blocks (RBs) [21]. Each RB constitutes two  $3 \times 3$  Conv layers with 64 feature maps, which are followed by ReLU activation and layer normalization [22]. The RBs are further followed by two  $1 \times 1$  Conv layers with 2 feature maps, whose output is reshaped back to vector form as  $\mathbf{h}^{(t+1)}$ .

We generate the training, validation, and testing datasets with 20000, 5000, and 5000 samples, respectively. The presented results are tested based on the testing dataset. FPN-OAMP is trained for 150 epochs based on the normalized MSE (NMSE) loss function using Adam optimizer. The minibatch size is 128 and the initial learning rate is 0.001. The learning rate is decayed by half at the end of every 40 epochs. During the training, validation, and testing processes, we set the maximum number of iterations of FPN-OAMP as 15. Other more detailed training settings that are omitted here can be found in [6].

### B. Noise Level Estimation

The accuracy of the noise level estimation can affect both the variance and the divergence terms in SURE, and is thus critical for the blind performance prediction. We provide the simulation results to verify the performance of the proposed PCA-based method. We first generate the complex-valued AWGN corrupted channels by using  $\tilde{\mathbf{h}}_{\text{noisy}} = \tilde{\mathbf{h}} + \tilde{\mathbf{m}}$  with  $\tilde{\mathbf{m}} \sim \mathcal{CN}(0, \sigma_{\tilde{\mathbf{m}}}^2 \mathbf{I}_N)$ , and then transform it into the equivalent real-valued form, i.e.,  $\mathbf{h}_{\text{noisy}} = \mathbf{h} + \mathbf{m}$ . We estimate the noise level  $\sigma_{\tilde{\mathbf{m}}}$  from the noisy channel  $\tilde{\mathbf{h}}_{\text{noisy}}$  or  $\mathbf{h}_{\text{noisy}}$ . The estimation is denoted by  $\hat{\sigma}_{\tilde{\mathbf{m}}}$ . The SNR is defined as  $1/\sigma_{\tilde{\mathbf{m}}}^2$ . Two benchmarks are compared:

- *Sparsity-based method*<sup>4</sup>: As said in Section III-A [13].
- *Oracle bound*<sup>5</sup>: Assume that the ground-truth channel  $\mathbf{h}$  is known, and estimate  $\sigma_{\tilde{\mathbf{m}}}$  directly from  $\mathbf{m} = \mathbf{h}_{\text{noisy}} - \mathbf{h}$  by the sample standard deviation, i.e.,  $\hat{\sigma}_{\tilde{\mathbf{m}}} = \sqrt{\frac{1}{N} \sum_{i=1}^{2N} (\mathbf{m})_i^2}$ .

In Table I, we present the performance of the noise level estimation with different noise levels. The bias, the standard deviation (std), and the root MSE (RMSE) of the noise level estimation are defined as  $\mathbb{E}[|\sigma_{\tilde{\mathbf{m}}} - \mathbb{E}[\hat{\sigma}_{\tilde{\mathbf{m}}}]|]$ ,  $\sqrt{\mathbb{E}[(\hat{\sigma}_{\tilde{\mathbf{m}}} - \mathbb{E}[\hat{\sigma}_{\tilde{\mathbf{m}}})^2]}$ , and  $\sqrt{\mathbb{E}[(\sigma_{\tilde{\mathbf{m}}} - \hat{\sigma}_{\tilde{\mathbf{m}}})^2]}$ , respectively. The bias and std respectively reflect the accuracy and the robustness of an estimator, while the RMSE reflects the overall performance. The virtual subarray size of the proposed method is set as  $5 \times 5$ , i.e.,  $d = 25$ . The runtime is tested using Matlab on Intel Core i7-9750H CPU.

From Table I, we observe that the proposed PCA-based method is highly accurate and robust. The RMSE performance is close to the oracle bound even though it does not have knowledge of the ground-truth channel. However, the performance of

<sup>4</sup>Since this benchmark was originally proposed for the complex Gaussian distribution [13], we test it using the complex-valued noisy channel  $\tilde{\mathbf{h}}_{\text{noisy}}$ .

<sup>5</sup>This is the minimum variance unbiased estimator of the oracle setting.

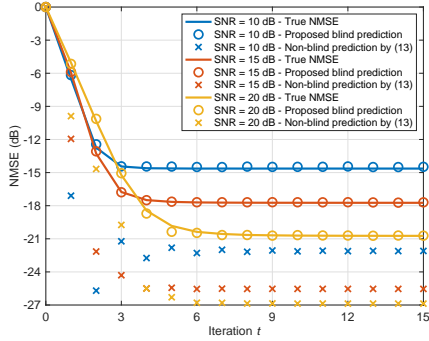


Fig. 3. Iterative behavior of the FPN-OAMP algorithm in terms of the true NMSE and predicted NMSE by different methods.

the sparsity-based method [13] is much worse, since the hybrid-field UM-MIMO channel does not satisfy the angular-domain sparsity [6]. On the contrary, the proposed PCA-based method does *not* rely on channel sparsity, and is thus applicable to a much broader class of channel models of practical interest. In addition, the runtime of the proposed method, though higher than the sparsity-based one, is within only a few milliseconds.

### C. Blind Performance Prediction

Since in practice we are more interested in normalized MSE (NMSE), it is presented instead by normalizing the predicted MSE with  $\|\mathbf{h}\|_2^2$ . If  $\|\mathbf{h}\|_2^2$  is unknown, we can approximate it by  $\|\mathbf{r}^{(t)}\|_2^2 - 2N\sigma_{\mathbf{e}^{(t)}}^2$ , as suggested in [13]. This can provide almost the same predicted NMSE as using the true channel power. We adopt this approximation in the following results.

To the best of our knowledge, this is the first attempt in this direction, and we can hardly find relevant baselines to compare with. For the sake of completeness, we provide a comparison with a *non-blind* and intuitive MSE performance prediction method commonly adopted in previous work [3], [15], i.e.,

$$\widehat{MSE}^{(t)} = 2N \max\left\{\frac{\|\mathbf{y} - \mathbf{M}\mathbf{h}^{(t)}\|_2^2 - Q_{\text{NRF}}\sigma_{\mathbf{n}}^2}{\text{tr}(\mathbf{M}^T\mathbf{M})}, \xi\right\}, \quad (13)$$

which requires the noise statistics, i.e.,  $\sigma_{\mathbf{n}}^2$  (oracle information). The predicted NMSE is obtained similarly by the normalization. This predictor is dependent on two much stronger assumptions on the distribution of  $\mathbf{r}^{(t)} - \mathbf{h}$  and  $\mathbf{h}^{(t)} - \mathbf{h}$  [3], [15], whose detailed explanation can be found in [3, Appendix B]. However, the DL-based NLE can often break these assumptions and make the predictor over-optimistic, or even return negative values for the predicted MSE [15]. To avoid unreasonable prediction, we set a floor value of  $\xi = 0.001$  according to [15].

In Fig. 3, we plot the true NMSE and the predicted NMSE as a function of the number of iterations  $t$ . The true NMSE is plotted with full line. The predicted NMSE by our blind method and the intuitive method using (13) is respectively plotted by circle and cross. It is observed that the predicted NMSE by our method agrees very well with the true NMSE, even though it is computed without using any oracle information. This confirms the accuracy of the proposed blind performance prediction method. By contrast, the prediction from the intuitive method using (13) is far away from the true performance. Furthermore, the runtime of the proposed method is low, taking only 0.031 seconds when tested in Pytorch on Intel Core i7-9750H CPU.

## V. CONCLUSION AND FUTURE WORK

This work proposed an efficient blind performance prediction method for DL-based UM-MIMO channel estimation. Accurate prediction can be achieved solely based on the received pilots, with no need of the ground-truth channel or any other oracle information. The predicted performance is useful for quantifying the uncertainty and identifying the potential risk of DL-based algorithms, which can serve as valuable design guidelines in practical deployment. For the future work, it is interesting to investigate how DL-based methods can adapt themselves when poor performance is detected based on the proposed framework.

## REFERENCES

- [1] K. B. Letaief, W. Chen, Y. Shi, J. Zhang, and Y.-J. A. Zhang, "The roadmap to 6G: AI empowered wireless networks," *IEEE Comm. Mag.*, vol. 57, no. 8, pp. 84–90, Aug. 2019.
- [2] K. B. Letaief, Y. Shi, J. Lu, and J. Lu, "Edge artificial intelligence for 6G: Vision, enabling technologies, and applications," *IEEE J. Sel. Areas Commun.*, vol. 40, no. 1, pp. 5–36, Jan. 2022.
- [3] H. He, C.-K. Wen, S. Jin, and G. Y. Li, "Model-driven deep learning for MIMO detection," *IEEE Trans. Signal Process.*, vol. 68, pp. 1702–1715, Feb. 2020.
- [4] Y. Ma, Y. Shen, X. Yu, J. Zhang, S. H. Song, and K. B. Letaief, "Learn to communicate with neural calibration: Scalability and generalization," *IEEE Trans. Wireless Commun.*, vol. 21, no. 11, pp. 9947–9961, Nov. 2022.
- [5] J. Zhang, X. Yu, and K. B. Letaief, "Hybrid beamforming for 5G and beyond millimeter-wave systems: A holistic view," *IEEE Open J. Commun. Soc.*, vol. 1, pp. 77–91, Jan. 2020.
- [6] W. Yu, Y. Shen, H. He, X. Yu, J. Zhang, and K. B. Letaief, "Hybrid far- and near-field channel estimation for THz ultra-massive MIMO via fixed point networks," in *Proc. IEEE Global Commun. Conf. (GLOBECOM)*, Rio de Janeiro, Brazil, Dec. 2022.
- [7] M. Borgerding, P. Schniter, and S. Rangan, "AMP-inspired deep networks for sparse linear inverse problems," *IEEE Trans. Signal Process.*, vol. 65, no. 16, pp. 4293–4308, Aug. 2017.
- [8] H. He, R. Wang, W. Jin, S. Jin, C.-K. Wen, and G. Y. Li, "Beam-space channel estimation for wideband millimeter-wave MIMO: A model-driven unsupervised learning approach," *IEEE Trans. Wireless Commun.*, to appear.
- [9] Y. Shen, J. Zhang, S. Song, and K. B. Letaief, "Graph neural networks for wireless communications: From theory to practice," *IEEE Trans. Wireless Commun.*, to appear.
- [10] X. Zheng and V. K. N. Lau, "Online deep neural networks for mmWave massive MIMO channel estimation with arbitrary array geometry," *IEEE Trans. Signal Process.*, vol. 69, pp. 2010–2025, Mar. 2021.
- [11] Q. Zou and H. Yang, "A concise tutorial on approximate message passing," *arXiv preprint arXiv:2201.07487*, 2022.
- [12] C. M. Stein, "Estimation of the mean of a multivariate normal distribution," *Ann. Statist.*, pp. 1135–1151, Nov. 1981.
- [13] A. Gallyas-Sanhueza and C. Studer, "Blind SNR estimation and nonparametric channel denoising in multi-antenna mmWave systems," in *Proc. IEEE Int. Conf. Commun. (ICC)*, Montreal, Canada, Jun. 2021.
- [14] R. Cao, H. He, X. Yu, J. Zhang, S. Song, Y. Gong, and K. B. Letaief, "Belief propagation for near-field cooperative localization and tracking in 6G vehicular networks," in *Proc. IEEE Int. Mediterr. Conf. Commun. Netw. (MeditCom)*, Athens, Greece, Sept. 2022.
- [15] J. Ma and L. Ping, "Orthogonal AMP," *IEEE Access*, vol. 5, pp. 2020–2033, Jan. 2017.
- [16] C. A. Metzler, A. Maleki, and R. G. Baraniuk, "From denoising to compressed sensing," *IEEE Trans. Inf. Theory*, vol. 62, no. 9, pp. 5117–5144, Sept. 2016.
- [17] W. Yu, Y. Shen, H. He, X. Yu, S. Song, J. Zhang, and K. B. Letaief, "An adaptive and robust deep learning framework for THz ultra-massive MIMO channel estimation," *arXiv preprint arXiv:2211.15939*, 2022.
- [18] T. Blu and F. Luisier, "The SURE-LET approach to image denoising," *IEEE Trans. Image Process.*, vol. 16, no. 11, pp. 2778–2786, Nov. 2007.
- [19] S. Ramani, T. Blu, and M. Unser, "Monte-Carlo Sure: A black-box optimization of regularization parameters for general denoising algorithms," *IEEE Trans. Image Process.*, vol. 17, no. 9, pp. 1540–1554, Sept. 2008.
- [20] G. Chen, F. Zhu, and P.-A. Heng, "An efficient statistical method for image noise level estimation," in *Proc. IEEE Conf. Comput. Vis. Pattern Recog. (CVPR)*, Boston, MA, USA, Jun. 2015.
- [21] K. He, X. Zhang, S. Ren, and J. Sun, "Deep residual learning for image recognition," in *Proc. IEEE Conf. Comput. Vis. Pattern Recog. (CVPR)*, Las Vegas, NV, USA, Jun. 2016.
- [22] J. L. Ba, J. R. Kiros, and G. E. Hinton, "Layer normalization," in *Proc. Adv. Neural Inf. Process. Syst. (NeurIPS)*, Barcelona, Spain, Dec. 2016.